

Small-angle X-ray scattering study on conformation of poly(sodium L-glutamate) in NaCl and NaF aqueous solutions

Shigeru Shimizu,^{a*} Yoshio Muroga,^b Tatsuya Hyono^a and Kimio Kurita^a

^aCollege of Science and Technology, Nihon University, Tokyo, 101-8308 Japan, and ^bGraduate School of Engineering, Nagoya University, Nagoya, 464-8603 Japan. Correspondence e-mail: shimizu@chem.cst.nihon-u.ac.jp

Received 16 August 2006
Accepted 6 February 2007

The effect of anions F^- and Cl^- on the conformation of poly(sodium L-glutamate) (PNaGA) in added-salt aqueous solution was studied using potentiometric titration, high-resolution proton nuclear magnetic resonance (NMR), circular dichroism (CD) and small-angle X-ray scattering (SAXS) techniques. In the titration curve for PNaGA in NaCl aqueous solution, four conformation regions, *i.e.* aggregation-, helical-, helix-to-coil transition- and random-coiled, were clearly observed but these regions were gradually obscured when the concentration of F^- was increased. Both CD and NMR spectra have clarified that the local conformation of PNaGA in NaF aqueous solution is a random-coiled state, independent of the degree of neutralization (DN). SAXS studies show that the conformation of a larger dimension for PNaGA having DN = 0.25 in 0.2 NaF aqueous solution is roughly mimicked by a worm-like chain having persistence length of *ca* 5.9 Å, but the conformation at DN = 0.80 is far from an isolated worm-like chain.

© 2007 International Union of Crystallography
Printed in Singapore – all rights reserved

1. Introduction

It is well known (Doty *et al.*, 1957) that poly(D- or L-glutamic acid) (PGA) in added-salt aqueous solution exhibits a conformational transition [helix-to-coil (H/C) transition] between the helical-state (H-state) and the coiled-state (C-state) by changing pH of the solution and, thus, PGA has attracted great interest (Zimm & Rice, 1960; Nagasawa & Holtzer, 1964; Muroga *et al.*, 1972; Olander & Holtzer, 1968) as a model for the phenomenon of folding or denaturation of proteins. As a result, the local structure in each of the conformational states has been well characterized. The structures in the H-state and the H/C-state are represented by interrupted helical chains and an averaged helical-sequence length in these states were evaluated by analyzing small-angle X-ray scattering (SAXS) data with the scattering function $P(q)$ for broken-rod-like chain model (Muroga *et al.*, 1988). The light scattering and intrinsic viscosity study (Hawkins & Holtzer, 1972) has shown that fully ionized PGA is represented by a random-coiled chain (worm-like chain) having an unperturbed effective bond length of 8 Å and a SAXS study (Shimizu *et al.*, 2007) has clarified counter-ion species dependence of the conformation of fully ionized PGA in aqueous solution.

However, the effect of anions F^- , Cl^- , Br^- and I^- on the local structure of poly(sodium L-glutamate) (PNaGA) has not been fully understood yet. The present work is devoted to comparing the effects of F^- and Cl^- on the structure of PNaGA in aqueous solution, using the potentiometric titration curve, high-resolution proton nuclear magnetic resonance (NMR), circular dichroism (CD) and SAXS techniques. These methods are expected to provide information on the local structures in different dimensions.

2. Experimental

2.1. Materials and potentiometric titration

The sodium salt of poly(L-glutamic acid) (PNaGA) of $M_w = 9.8 \times 10^4$ was purchased from Sigma–Aldrich Chemical Co. PNaGA was converted to the acid form by passing it through a column filled with a mixed bed of the ion exchange resins, Amberlite IR-120B and IR-400.

The potentiometric titration of PLGA was carried out at an added-salt concentration C_s of 0.2 M under an N_2 atmosphere at room temperature with SevenMulti S40 pH meter (Mettler Toledo Co.). The polymer concentration C_p was 0.01 g cm^{-3} .

2.2. SAXS measurement

The SAXS measurements were performed at the beamline BL-10C of the Photon Factory of High Energy Accelerator Research Organization, Tsukuba, Japan. The wavelength of an incident X-ray beam, λ , was monochromated to 1.488 Å and the sample-to-detector distance was *ca* 1 m. The exact camera distance was calibrated using a 6th-peak of chicken tendon collagen (corresponding interplanar spacing of lattice plane, $d = 653 \text{ Å}$). The scattered X-rays are detected on a position-sensitive proportional counter with 512 channels. The details of the spectrometer specification and measurement procedure were described in reference (Ueki *et al.*, 1982/1983). Since the size of the X-ray beam at the sample position was so small compared with the camera length that the system could be regarded as a point-focusing system, both corrections of slit-length and slit-width were safely neglected. The sample cell was made of stainless steel and had quartz windows of 20 μm thickness at an interval of 1 mm. The excess

scattering intensity of the sample over the solvent was determined after transmission corrections for both solution and solvent. The scattering data were registered over the modulus of the scattering vector q , ranging from 0.01 \AA^{-1} to 0.3 \AA^{-1} , where q is defined as $(4\pi/\lambda)\sin(\theta/2)$ where λ is the X-ray wavelength and θ is the scattering angle.

2.3. CD and ^1H NMR measurement

The circular dichroism spectrum was measured with a JASCO J-720 spectrometer, using the cell of path length 1.0 mm. ^1H NMR experiments were performed on a Jeol Model JNM-GX400 spectrometer. C_s was kept at 0.2 M for all measurements. C_p is less than 0.001 g cm^{-3} for CD and 0.01 g cm^{-3} for ^1H NMR and measuring temperature is room temperature.

3. Results and discussion

3.1. Potentiometric titration

Fig. 1 shows the potentiometric titration data for PGA in aqueous solution involving a mixture of added-salts, NaCl and NaF, where total C_s was kept at 0.2 M and only the ratio varied. The data are plotted in the form of $-\log K_a$, $pK_a [= \text{pH} + \log\{(1-\alpha)/\alpha\}]$ vs α , where K_a is apparent dissociation constant and α is degree of neutralization. In 0.2 M NaCl aqueous solution, the potentiometric titration curve is divided into four regions: (A) aggregation, (B) helix, (C) helix/coil transition and (D) random-coil regions, as is well established (Wada, 1960; Nagasawa & Holtzer, 1964). However, the presence of F^- remarkably deforms the titration curve and the four conformational regions are no longer discriminated when a mixture of 0.05 M NaF and 0.15 M NaCl is employed as an added-salt. Such a characteristic effect of F^- on the titration curve of PGA has not been observed in the presence of other halide ions, Cl^- , Br^- and I^- .

3.2. ^1H NMR

Fig. 2 shows ^1H NMR spectra of PNaGA in NaCl/ D_2O solution at $\alpha = 0.25$ (A) and 0.86 (B), and PNaGA in NaF/ D_2O solution at $\alpha =$

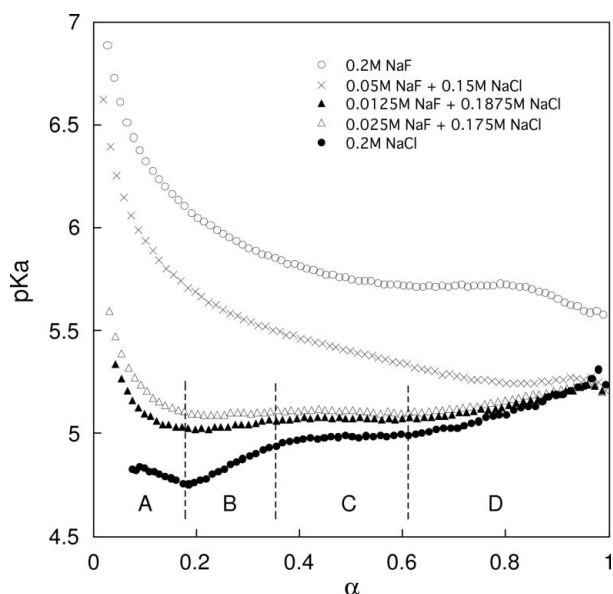


Figure 1 Potentiometric titration curves for PNaGA in different added-salt solutions. The curve for PNaGA in NaCl is divided into regions: (A) aggregation, (B) helix, (C) helix/coil transition, (D) random coiled.

0.25 (C) and 0.86 (D). In the (B), (C) and (D) spectra, two peaks centered at *ca* 1.75 and 1.8 p.p.m. and a single peak centered at *ca* 2.1 p.p.m. are assigned to $\beta\text{-CH}_2$ protons and $\gamma\text{-CH}_2$ protons, respectively, of PNaGA in the random-coiled state (Markley *et al.*, 1967; Tsutsumi *et al.*, 1978). The three peaks in the A spectra are assigned to CH_2 protons of PNaGA in the helical state, but the assignment of each peak was not made here. From a comparison of these four spectra, it is suggested that PNaGA in NaF aqueous solution takes a local conformation of random coil, independent of α .

3.3. CD

Fig. 3 shows the CD spectra of PNaGA in 0.2 M NaCl aqueous solution at $\alpha = 0.25$ (A) and $\alpha = 0.86$ (B), and PNaGA in 0.2 M NaF aqueous solution at $\alpha = 0$ (C), $\alpha = 0.25$ (D), $\alpha = 0.80$ (E) and $\alpha = 0.80$ (F; $C_s = 0.1 \text{ M}$). As is well established, CD spectrum of PNaGA in the helical state exhibit two negative extreme near 209 and 222 nm and a positive extreme near 191 nm, and these characteristic extremes would disappear in the random-coiled state (Fasman, 1967; Walton, 1981). From a comparison of the CD spectra, it is further confirmed that PNaGA in 0.2 M NaF aqueous solution takes a local conformation of random coil over an entire range of α .

3.4. SAXS

As C_s is lowered, generally speaking, electrostatic interactions between different polyelectrolyte chains are accentuated and they could appear as a peak or a broad hump (Nierlich *et al.*, 1979; Matsuoka & Ise, 1994) in a low- q range in the SAXS curve, plotted in the form $I(q)$ vs q , where $I(q)$ is observed scattering intensity. As is shown in Fig. 4, however, the SAXS curves for PNaGA at $\alpha = 0.25$ and 0.86 in 0.2 M NaCl and at $\alpha = 0.25$ in 0.2 M NaF aqueous solution show no such humps, indicating that the intermolecular interactions could be safely neglected, at least, under these conditions. At $\alpha = 0.80$ in 0.2 M NaF aqueous solution, however, the SAXS curve seems to have a hump in the small q range. C_p is 0.01 g cm^{-3} and the temperature is 298 K for all samples.

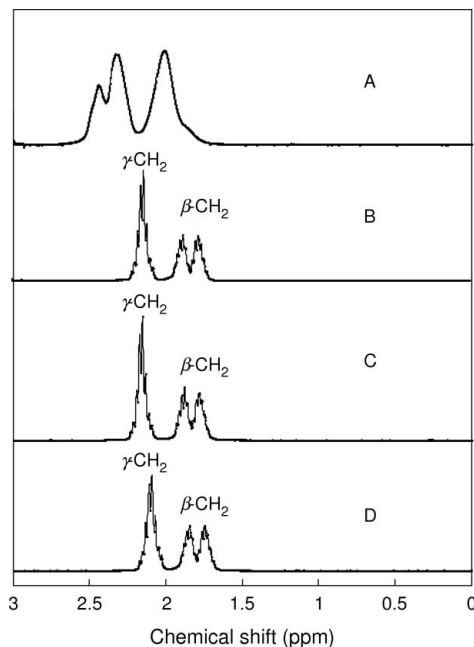


Figure 2 ^1H NMR spectrum for PNaGA in NaCl and NaF. Experimental data for (A), (B), (C) and (D) are given in text.

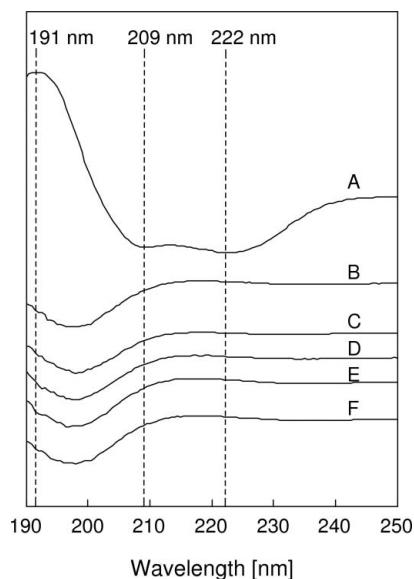


Figure 3
CD spectra for PNaGA in NaCl and NaF. Experimental data for (A), (B), (C) and (D) are given in the text. In addition, (A) pH 4.32; (B) pH 6.99; (C) pH 5.44; (D) pH 5.70; (E) pH 6.53; (F) pH 6.31.

As is well established, the local structure of a polymer chain can be regarded as rod-like chain in q range:

$$\frac{1}{L_p^2} < q^2 < \frac{1}{\langle R_{cs}^2 \rangle}, \quad (1)$$

where L_p and $\langle R_{cs}^2 \rangle$ are the persistence length and the mean-square radius of the cross-section of the polymer chain, respectively. In the q range given by equation (1), the scattering intensity is expressed by (Porod, 1982):

$$I(q) \sim I_{\text{thin}}(q)I_{\text{cs}}(q), \quad (2)$$

where $I_{\text{thin}}(q)$ is the scattering intensity from a needle with no cross-section, which is proportional to $1/q$, and $I_{\text{cs}}(q)$ is the scattering intensity from the cross-section of the rod:

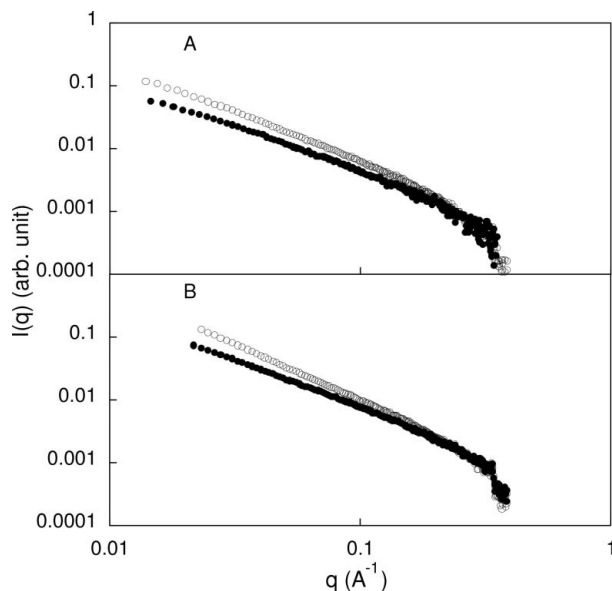


Figure 4
The scattering profile of PNaGA in 0.2 M NaCl and in NaF. (A) NaCl, open circle: $\alpha = 0.25$, filled circle: $\alpha = 0.86$; (B) NaF, open circle: $\alpha = 0.25$, filled circle: $\alpha = 0.80$.

Table 1
Observed molecular parameters evaluated from SAXS curves.

System	α	$\langle R_{cs}^2 \rangle^{1/2}$ (Å)	L_p (Å)
0.2 M NaCl	0.86	4.0 ± 0.5	6.0 ± 0.5
0.2 M NaF	0.25	4.0 ± 0.5	5.9 ± 0.5
0.2 M NaF	0.80	4.0 ± 0.5	4.7 ± 0.5

$$I_{\text{cs}}(q) \sim \exp\left(-\frac{1}{2}\langle R_{cs}^2 \rangle q^2\right). \quad (3)$$

Accordingly, $\langle R_{cs}^2 \rangle$ of a polymer chain is evaluated from the slope of a cross-section plot, $\ln[I(q)q]$ vs q^2 , in q range given by equation (1).

Fig. 5 shows the cross-section plot for PNaGA. As is shown by the solid line in the figure, the data points form a straight line in q range of equation (1) and the slope gives $\langle R_{cs}^2 \rangle^{1/2}$ of 4.0 ± 0.5 Å (Table 1) independently of α and added-salt species. The magnitude of $\langle R_{cs}^2 \rangle^{1/2}$ thus obtained is comparable with the realistic one of PNaGA having side chains in extended form, which is 6.4 Å and 4.9 Å in a helical form and in a random-coiled form, respectively, involving the diameter of sodium ion, 2.5 Å (Muroga *et al.*, 1972).

Fig. 6 shows the Kratky plot, $P(q)q^2$ vs q , for (A) PNaGA in 0.2 M NaCl aqueous solution at $\alpha = 0.86$, (B) PNaGA in 0.2 M NaF aqueous solution at $\alpha = 0.25$ and (C) at $\alpha = 0.86$, and (D) PGA in *N*-methyl

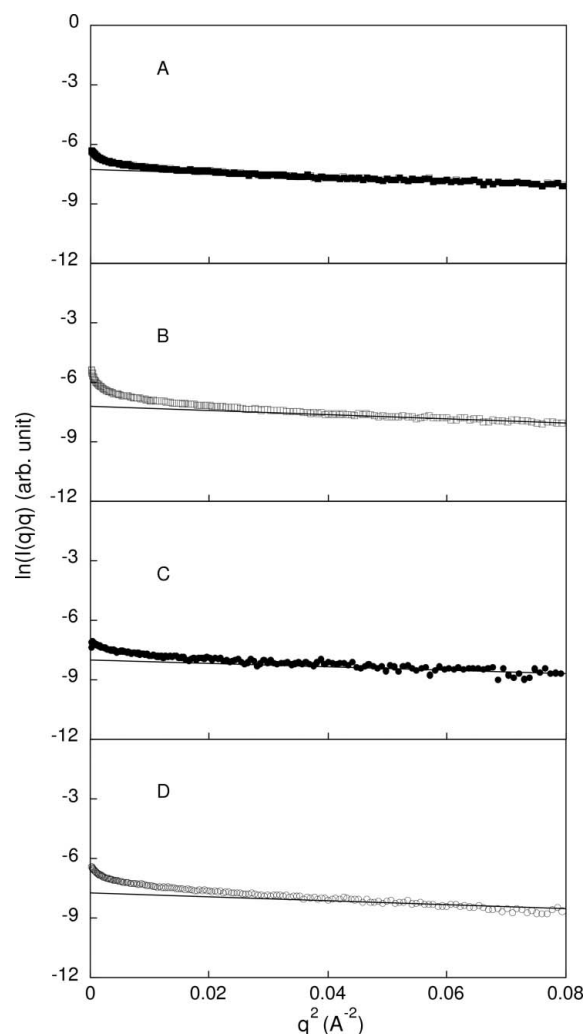


Figure 5
Cross-section plot of PNaGA in 0.2 M NaCl [(A) $\alpha = 0.25$, (B) $\alpha = 0.86$] and 0.2 M NaF [(C) $\alpha = 0.25$, (D) $\alpha = 0.8$]. C_p is 0.01 g cm^{-3} and measured at 298 K for all samples.

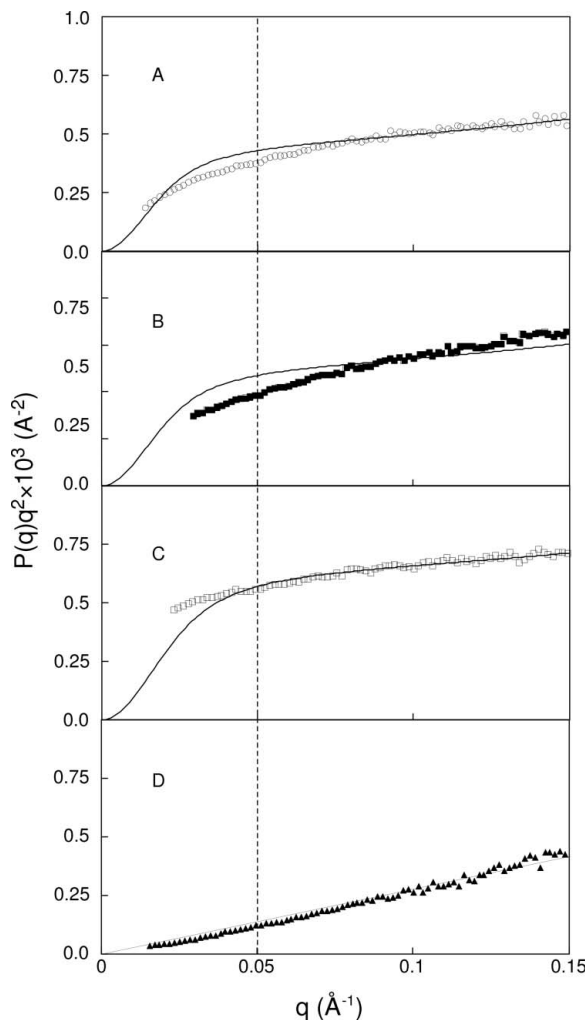


Figure 6 Kratky plot for PNaGA ($C_p = 0.01 \text{ g cm}^{-3}$, 298 K). Data for (A), (B), (C) and (D) are given in text. (D) has $C_s = 0.026 \text{ g cm}^{-3}$ and measured at 333 K. The solid curves in (A), (B) and (C) are theoretical computed with the scattering function of the worm-like chain.

acetamide (NMA) at $\alpha = 0$, where $P(q)$ was evaluated by $I(q)/I(0)$, and $I(0)$ is the scattering intensity extrapolated to $q = 0$, which was determined by Guinier approximation. It is seen that the plots of (A) [random-coil chain (Nagasawa & Holtzer, 1964)] and (D) [helical chain (Nagasawa & Holtzer, 1964)] well coincide with theoretical prediction that the plot for a random-coiled chain should be represented by a convex curve, whereas the plot for a helical chain by a straight line passing through an origin. Here, it was confirmed that the effect of C_p on the plot is substantially negligible for SAXS data of PNaGA in 0.2 M NaCl aqueous solution (Shimizu *et al.*, 2007). It is seen that the plots (A), (B) and (C) resemble each other and thus they were compared with theoretical scattering intensity $I_{wm}(q)$ for a worm-like chain having thickness $(R_{cs}^2)^{1/2}$. $I_{wm}(q)$ is given by $P_{wm}(q)\exp(-\frac{1}{2}(R_{cs}^2)^{1/2}q^2)$, where $P_{wm}(q)$ is the scattering function for a worm-like chain, analytically derived by Sharp and Bloomfield (Sharp & Bloomfield, 1968; Schmid *et al.*, 1971):

$$P_{wm}(q) = 2u^{-2}[\exp(-u) - 1 + u] + \frac{4}{15L_r} + \frac{7}{15L_r u} - \left[\frac{11}{15L_r} + \frac{7}{15L_r u} \right] \exp(-u), \quad (4)$$

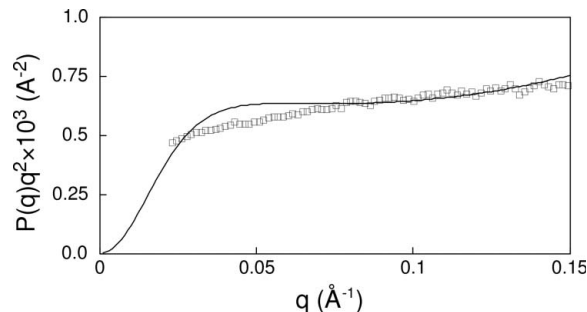


Figure 7 Kratky plot of PNaGA ($\alpha = 0.8$) in 0.2 M NaF. Solid curve is theoretical one computed with the scattering function of the dendrimer.

where u and L_r are defined by the contour length of a polymer chain L_c and the persistence length L_p as

$$u = L_c L_p q^2 / 3, \quad (5)$$

$$L_r = L_c / 2L_p. \quad (6)$$

Equation (4) is valid under the conditions,

$$L_r > 10 \quad \text{and} \quad (2L_p q)^2 < 10. \quad (7)$$

The solid curves in (A), (B) and (C) of Fig. 6 are theoretical ones computed with $P_{wm}(q)$ assuming $L_c = 1990 \text{ \AA}$ and $L_p = 5.9 - 6.0 \pm 0.5 \text{ \AA}$. In the plots (A) and (B), the agreement between the observed and the theoretical data is fairly satisfactory except in low- q range, where the observed data downward deviates from the theoretical one. The reason for such a downward deviation might be due to fairly broad molecular-weight-distribution of PNaGA and/or possible excluded-volume effect. The magnitude of $L_p = 5.9 - 6.0 \pm 0.5 \text{ \AA}$ thus obtained is comparable with L_p corresponding to an unperturbed effective bond-length of 8 \AA (Hawkins & Holtzer, 1972), *ca* 4 \AA.

On the other hand, the observed data in the plot (C) slightly deviate upwards from the theoretical curve in q range lower than 0.05 \AA^{-1} , suggesting that, for PNaGA at $\alpha = 0.80$ in 0.2 M NaF, intermolecular interactions could not be neglected or segment density within a polymer coil might be higher compared with that in a random-coiled chain, or both. The requirement for high segment density might be satisfied by a swollen gel having a network structure. From this consideration, a scattering function $P_{gel}(q)$ for a gel consisting of regular multi-branches, so-called dendrimer, was applied for analyzing the plot of (C), which was developed by Hammouda (Hammouda, 1992). The dendrimer is formed of N_b branches and each branch is composed of N generations of monomer blocks. The number of blocks is multiplied by a factor f (functionality parameter) in going from one generation to the next. Each block is formed with n monomer links having segment length b . The solid curve in Fig. 7 is a theoretical curve for the dendrimer, computed with $b = 20 \text{ \AA}$, $N = 2$, $N_b = 2$, $f = 2$ and $n = 10$. Discrepancy between the observed curve and theoretical curve was little improved in low- q range. Anyway, it seems certain that the conformation of PNaGA at $\alpha = 0.8$ in NaF aqueous solution is far apart from the conformation of an isolated worm-like chain.

4. Conclusion

Based on the results obtained from the potentiometric titration, high-resolution proton NMR, circular dichroism (CD) and small-angle X-ray scattering (SAXS) techniques, the effect of anions F^- and Cl^-

on the conformation of poly(sodium L-glutamate) (PNaGA) in added-salt aqueous solution has been discussed. NMR and CD studies show that the local conformation for PNaGA in NaCl aqueous solution clearly depends on the degree of neutralization (DN) and it takes a helical state at low DN and a random-coiled state at high DN, but the local conformation of PNaGA in NaF aqueous solution is a random-coiled state independent of the DN. On the other hand, the SAXS study shows that the conformation of PNaGA at $\alpha = 0.25$ in 0.2 M NaF aqueous solution is roughly mimicked by a worm-like chain having persistence length of *ca* 5.9 Å, but the conformation at $\alpha = 0.80$ is far from an isolated worm-like chain.

This work was partly supported by Nihon University Research Grant for 2005.

References

- Doty, P. A., Wada, A. & Yang, J. T. (1957). *J. Polym. Sci.* **23**, 851–861.
- Fasman, G. D. (1967). Editor. *Poly α -Amino Acids*. New York: Marcel Dekker, Inc.
- Hammouda, B. (1992). *J. Polym. Sci. Part B Polym. Phys.* **30**, 1387–1390.
- Hawkins, R. B. & Holtzer, A. (1972). *Macromolecules*, **5**, 294–301.
- Markley, J. L., Meadows, D. H. & Jardetzky, O. (1967). *J. Mol. Biol.* **27**, 25–40.
- Matsuoka, H. & Ise, N. (1994). *Adv. Polym. Sci.* **114**, 187–231.
- Muroga, Y., Suzuki, K., Kawaguchi, Y. & Nagasawa, M. (1972). *Biopolymers*, **11**, 137–144.
- Muroga, Y., Tagawa, H., Hiragi, Y., Ueki, T., Kataoka M., Izumi, Y. & Amemiya, Y. (1988). *Macromolecules*, **21**, 2756–2760.
- Nagasawa, M. & Holtzer, A. (1964). *J. Am. Chem. Soc.* **86**, 538–543.
- Nierlich, M., William, C. E., Boue, F., Cotton, J. J. P., Daoud, M., Farnoux, B., Jannink, G., Picot, C., Moan, M., Wolff, C., Rinaudo, M. & de Gennes, P. G. (1979). *J. Phys. (Paris)*, **40**, 701–704.
- Olander, D. S. & Holtzer, A. (1968). *J. Am. Chem. Soc.* **90**, 4549–4560.
- Porod, G. (1982). *Small Angle X-ray Scattering*, edited by O. Glatter & O. Kratky. New York: Academic Press.
- Schmid, C. W., Rinehart, F. P. & Hearst, J. E. (1971). *Biopolymers*, **10**, 883–893.
- Sharp, P. & Bloomfield, V. A. (1968). *Biopolymers*, **6**, 1201–1211.
- Shimizu, S., Muroga, Y., Miyahara, M., Iida, S., Ishibashi, M. & Kurita, K. (2007). In preparation.
- Tsutsumi, A., Perly, B., Forchioni, A. & Chachaty, C. (1978). *Macromolecules*, **11**, 977–986.
- Ueki, T., Hiragi, Y., Izumi, Y., Tagawa, H., Kataoka, M., Muroga, Y., Matsushita, T. & Amemiya, Y. (1982/1983). Photon Factory Activity Report VI70–VI71.
- Wada, A. (1960). *J. Mol. Phys.* **8**, 409–416.
- Walton, A. G. (1981). *Polypeptides and Protein Structure*. New York: Elsevier.
- Zimm, B. H. & Rice, S. A. (1960). *Mol. Phys.* **3**, 391–407.